

Part II. Algebraic Tails in Three-Dimensional Quantum Plasmas

We review various exact results concerning the presence of algebraic tails in three-dimensional quantum plasmas. First, we present a solvable model of two quantum charges immersed in a classical plasma. The effective potential between the quantum charges is shown to decay as $1/r^6$ at large distances r . Then, we mention semiclassical expansions of the particle correlations for charged systems with Maxwell-Boltzmann statistics and short-ranged regularization of the Coulomb potential. The quantum corrections to the classical quantities, from order \hbar^4 on, also decay as $1/r^6$. We also give the result of an analysis of the charge correlation for the one-component plasma in the framework of the usual many-body perturbation theory; some Feynman graphs beyond the random phase approximation display algebraic tails. Finally, we sketch a diagrammatic study of the correlations for the full many-body problem with quantum statistics and pure $1/r$ interactions. The particle correlations are found to decay as $1/r^6$, while the charge correlation decays faster, as $1/r^{10}$. The coefficients of these tails can be exactly computed in the low-density limit. The absence of exponential screening arises from the quantum fluctuations of partially screened dipolar interactions.

KEY WORDS: Coulomb systems; quantum statistical mechanics; correlations; algebraic tails; screening.

1. INTRODUCTION

We consider a quantum nonrelativistic multicomponent plasma of point charges. Each species α of particles is characterized by a charge e_α , a mass m_α , and a spin S_α . This system describes matter under usual conditions, where the fundamental constituents are electrons and nuclei interacting via electrostatic Coulomb interaction. The quantum Hamiltonian of the system is

$$H = -\sum_i \frac{\hbar^2}{2m_i} \Delta_i + \frac{1}{2} \sum_{i \neq j} e_i e_j v_c(|\mathbf{r}_i - \mathbf{r}_j|). \quad (1.1)$$

In (1.1), the first term is the nonrelativistic kinetic energy of the particles, while $v_c(r)$ is the pure Coulomb potential in three dimensions

$$v_c(r) = \frac{1}{r}. \quad (1.2)$$

The quantum fluctuations together with Fermi statistics ensure that the system does not implode, as shown by Dyson and Lenard.⁽¹⁾ (At least all species with a given sign are fermions). On the other hand, the local neutrality makes screening effects possible, so that the system does not explode, as shown by Lieb and Lebowitz.⁽²⁾ Thus, the quantum non-relativistic plasma has a well-behaved thermodynamic limit.⁽²⁾ In other words, matter at our scale, where Coulomb interactions are most dominant, is stable.

In this brief review, we are interested in the large-distance behavior of the static internal correlations. Since matter is stable, an integrable decay is expected. The usual self-consistent approximations, which are valid in weak coupling regimes, such as the classical Debye–Hückel theory,⁽³⁾ the semiclassical Thomas–Fermi model,⁽⁴⁾ and the Random Phase Approximation⁽⁵⁾ (RPA) for quantum plasmas at high density, have led to the common belief that the static correlations decay exponentially at large distances. However, these mean-field predictions need to be settled on firmer grounds. It turns out that, in the classical case, the rigorous results are in agreement with the picture of Debye screening: an exponential clustering of the correlations in the weak-coupling limit was established by Brydges and Federbush.⁽⁶⁾ Nevertheless, in the quantum case, strong doubts about an exponential fall-off were first raised in ref. 7. Then, Brydges and Seiler⁽⁸⁾ found that an infinite correlation length appears in some imaginary-time Green functions. They conjectured that an external charge is not exponentially screened and that, in nearly classical regimes, the exponential decay would be very close to the truth for all but extremely large distances.

We present various recent results showing that algebraic decay of the correlations does appear in quantum plasmas. In Section 2, we describe a simple model consisting of two quantum charges immersed in a classical plasma.⁽⁹⁾ The effective potential between the two quantum charges is shown to decay as $1/r^6$. In Section 3, we summarize various attempts to treat the full many-body problem. The same algebraic fall-off as in the model also arises in semiclassical expansions with Maxwell–Boltzmann statistics^(10,9) and in some corrections to the Random Phase Approximation for the One-Component Plasma (OCP).⁽¹¹⁾ The full many-body problem with quantum statistics and pure $1/r$ interactions is presented in Section 4. Diagrammatic expansions show the existence of a $1/r^6$ decay of the particle–particle correlation,^(12,13,14) and provide the exact form of the algebraic tails at low densities.⁽¹⁵⁾ We stress that these algebraic decays of the correlations are sufficiently fast to be compatible with the basic screening rules.⁽¹⁶⁾ For instance, the charge of the polarization cloud around an infinitesimal external charge exactly compensates the latter charge.

2. A SIMPLE MODEL: TWO QUANTUM CHARGES IN A CLASSICAL PLASMA

We consider two quantum point charges, with mass $m_1(m_2)$ and charge $e_1(e_2)$, immersed in a classical plasma. For a given configuration $\{\mathbf{R}_N\}$ of the classical plasma, the Hamiltonian of the system reads

$$H = -\frac{\hbar^2}{2m_1} \Delta_1 - \frac{\hbar^2}{2m_2} \Delta_2 + V_C(\mathbf{r}_1, \mathbf{r}_2, \mathbf{R}_N). \quad (2.1)$$

In (2.1), the first two terms are the kinetic energies of the quantum charges and V_C is the Coulomb interaction energy of all charges. The kinetic energies of the classical charges are not included in (2.1), because they do not contribute to the quantities of interest, which are defined as equilibrium averages over the configurations $\{\mathbf{R}_N\}$ of the classical plasma.

The effective potential ϕ_{eff} between the two quantum charges is defined as the difference between the excess free energy F_2 when the pair is immersed in the classical bath and the excess free energy F_1 of the particles when they are separately immersed in the classical bath,

$$\phi_{\text{eff}}(|\mathbf{r}_2 - \mathbf{r}_1|) = F_2(\mathbf{r}_2, \mathbf{r}_1) - F_1(\mathbf{r}_2) - F_1(\mathbf{r}_1). \quad (2.2)$$

For instance, F_2 reads

$$F_2(\mathbf{r}_2, \mathbf{r}_1) = -k_B T \ln \left[\frac{\int d\mathbf{R}_N (2\pi\lambda_1^2)^{3/2} (2\pi\lambda_2^2)^{3/2} \langle \mathbf{r}_1 \mathbf{r}_2 | \exp(-\beta H) | \mathbf{r}_1 \mathbf{r}_2 \rangle}{\int d\mathbf{R}_N \exp(-\beta U_C(\mathbf{R}_N))} \right] \quad (2.3)$$

where U_C is the Coulomb interaction energy of the classical charges, and λ_i is the de Broglie length $\lambda_i \equiv \sqrt{\beta\hbar^2/m_i}$. It is assumed that the classical bath is in a fluid phase invariant under translations and rotations. (The classical bath is either an OCP or a multicomponent plasma with short-ranged regularization of the Coulomb potential.)

In order to study the large-distance behavior of ϕ_{eff} , it is particularly convenient to use the Feynman–Kac representation of the matrix element in (2.3), as described in Section 2.1.

2.1. The Charged Classical Filament Impurities

According to the Feynman–Kac formula, the diagonal element of the density-matrix for the two quantum particles can be written as

$$\begin{aligned} \langle \mathbf{r}_1 \mathbf{r}_2 | \exp(-\beta H) | \mathbf{r}_1 \mathbf{r}_2 \rangle &= \frac{1}{(2\pi\lambda_1^2)^{3/2} (2\pi\lambda_2^2)^{3/2}} \int \mathcal{D}(\xi_1) \mathcal{D}(\xi_2) \\ &\times \exp \left[-\beta \int_0^1 ds V_C(\mathbf{r}_1 + \lambda_1 \xi_1(s), \mathbf{r}_2 + \lambda_2 \xi_2(s), \mathbf{R}_N) \right] \end{aligned} \quad (2.4)$$

In (2.4), the dimensionless vector functions ξ_1 and ξ_2 represent Brownian paths which vanish at times $s=0$ and $s=1$, and $D(\xi)$ is the normalized Gaussian measure with covariance,

$$\int \mathcal{D}(\xi) \xi_\mu(s) \xi_\nu(t) = \delta_{\mu\nu} \inf(s, t) [1 - \sup(s, t)]. \quad (2.5)$$

The formula (2.4) allows one to introduce a natural correspondence between the two quantum particles and two classical filaments \mathcal{F}_1 and \mathcal{F}_2 , which are defined by their positions \mathbf{r}_i and their shapes $\lambda_i \xi_i$ (see Fig. 6). In this equivalence, the two-body density matrix is exactly given by functional integration of a Boltzmann factor over the shapes of the filaments \mathcal{F}_i weighted by the Gaussian measures $D(\xi_i)$.

The crucial point is that the potential between the two closed filaments \mathcal{F}_1 and \mathcal{F}_2 in the vacuum is not equal to the electrostatic interaction energy between two uniformly charged wires with the same positions and shapes.

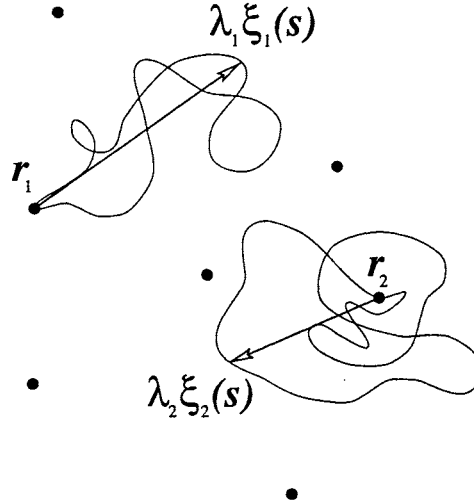


Fig. 6. The two classical filaments \mathcal{F}_i with positions \mathbf{r}_i and shapes $\lambda_i \xi_i(s)$, ($i=1, 2$), immersed in a bath of classical charges represented by black circles.

Thus, the interaction in the Maxwell–Boltzmann factor associated with the filaments \mathcal{F}_1 and \mathcal{F}_2 can be decomposed as follows,

$$\int ds V_C(\mathbf{r}_1 + \lambda_1 \xi_1(s), \mathbf{r}_2 + \lambda_2 \xi_2(s), \mathbf{R}_N) = U^{\text{elect}}(\mathcal{F}_1, \mathcal{F}_2, \mathbf{R}_N) + W(\mathcal{F}_1, \mathcal{F}_2). \quad (2.6)$$

The first term is the electrostatic interaction energy of the whole classical system made of the two charged wires immersed in the bath. The second term $W(\mathcal{F}_1, \mathcal{F}_2)$ is a purely quantum contribution. The latter is equal to the difference between the interaction in the vacuum between the filaments which appears in the Feynman–Kac formula, on the one hand, and the usual electrostatic interaction in the vacuum between uniformly charged wires, on the other hand,

$$W(\mathcal{F}_1, \mathcal{F}_2) = e_1 e_2 \int_0^1 ds_1 \int_0^1 ds_2 [\delta(s_1 - s_2) - 1] \times v_C(|\mathbf{r}_1 + \lambda_1 \xi_1(s) - \mathbf{r}_2 - \lambda_2 \xi_2(s)|). \quad (2.7)$$

When using the Feynman–Kac formula (2.4) in the definition (2.3) combined with the decomposition (2.6), the fact that W does not depend on the classical configurations $\{\mathbf{R}_N\}$ leads to

$$\phi_{\text{eff}}(|\mathbf{r}_2 - \mathbf{r}_1|) = -k_B T \ln \left[\int \bar{\mathcal{D}}(\xi_1) \bar{\mathcal{D}}(\xi_2) \times \exp(-\beta(\phi_{\text{eff}}^{\text{elect}}(\mathcal{F}_1, \mathcal{F}_2) + W(\mathcal{F}_1, \mathcal{F}_2))) \right] \quad (2.8)$$

where $\bar{\mathcal{D}}(\xi)$ is the effective measure

$$\bar{\mathcal{D}}(\xi_i) = \mathcal{D}(\xi_i) \frac{\exp(-\beta F_i^{\text{elect}}(\mathcal{F}_i))}{\exp(-\beta F_1(\mathbf{r}_i))} \quad (2.9)$$

in which F_i^{elect} is the excess free energy of the charged wire associated with the filament \mathcal{F}_i immersed in the classical bath. Moreover, $\phi_{\text{eff}}^{\text{elect}}(\mathcal{F}_1, \mathcal{F}_2)$ is the effective potential between the charged wires associated with \mathcal{F}_1 and \mathcal{F}_2 . (The definition is similar to (2.2).)

2.2. Absence of Exponential Screening

According to rigorous results, the effective potential $\phi_{\text{eff}}^{\text{elect}}$ between two charged wires decays exponentially when the distance between the wires

becomes very large compared with their extents. On the other hand, the purely quantum term W decays algebraically as a $1/r^3$ dipolar-like interaction,

$$W(\mathcal{F}_1, \mathcal{F}_2) \sim e_1 e_2 \int_0^1 ds_1 \int_0^1 ds_2 [\delta(s_1 - s_2) - 1] \\ \times (\lambda_1 \xi_1(s_1) \cdot \nabla_1) (\lambda_2 \xi_2(s_2) \cdot \nabla_2) \frac{1}{|\mathbf{r}_1 - \mathbf{r}_2|}. \quad (2.10)$$

The $1/r$ and $1/r^2$ terms in the large- r expansion of W vanish, because the monopole–monopole and monopole–multipole parts of the interaction between the filaments coincide with their electrostatic counterparts between the charged wires. Since the renormalized measure $\bar{\mathcal{D}}(\xi)$ decays faster than any inverse power of $|\xi|$ for large filaments, the leading terms in the large-distance behavior of the effective potential $\phi_{\text{eff}}(\mathbf{r}_1, \mathbf{r}_2)$ are given by the expansion of the sole Boltzmann factor $\exp[-\beta W]$ with respect to W in formula (2.8). After integration over the random shapes of the filaments, the harmonicity of the Coulomb potential turns all the *a priori* algebraic contributions from W into short-ranged terms. Thus, the first leading term is given by

$$\phi_{\text{eff}}(|\mathbf{r}_2 - \mathbf{r}_1|) \sim -\frac{\beta}{2} \int \bar{\mathcal{D}}(\xi_1) \bar{\mathcal{D}}(\xi_2) [W(\mathcal{F}_1, \mathcal{F}_2)]^2, \quad |\mathbf{r}_2 - \mathbf{r}_1| \rightarrow \infty, \quad (2.11)$$

where W itself is replaced by its asymptotic form (2.10).

Finally, as shown by Eq. (2.11), the effective potential $\phi_{\text{eff}}(|\mathbf{r}_1 - \mathbf{r}_2|)$ decays as

$$\phi_{\text{eff}}(|\mathbf{r}_1 - \mathbf{r}_2|) \sim \frac{\text{const}}{|\mathbf{r}_1 - \mathbf{r}_2|^6}, \quad |\mathbf{r}_2 - \mathbf{r}_1| \rightarrow \infty. \quad (2.12)$$

The coefficient of the $1/r^6$ algebraic tail in (2.12) is always negative. In general, it depends on the thermodynamic parameters of the classical plasma, and it can be explicitly computed for weakly coupled systems (Debye–Hückel regime).⁽⁹⁾ This simple model exhibits a fundamental phenomenon: the fluctuations of the purely quantum potential W cannot be screened by the classical plasma. Thus, contrarily to the classical case, the screening is only algebraic.

3. TOWARDS THE TRUE PROBLEM

3.1. Semiclassical Expansions

A first breakthrough towards the description of correlations in quantum plasmas was obtained via Wigner–Kirkwood (WK) expansions in powers of \hbar^2 . Such expansions can be safely used for the OCP, since this model has a well-behaved classical limit.^(17, 18) The WK expansion of the charge correlation of the OCP was first studied by Jancovici.⁽¹⁹⁾ He showed that the first quantum correction of order \hbar^2 decays exponentially fast, as does the purely classical term. More recently, the next correction of order \hbar^4 was found to decay algebraically as,^(10, 9)

$$\frac{7}{16\pi^2} \frac{\beta^2 \hbar^4 e^2}{m^2} \frac{1}{r^{10}}. \quad (3.1)$$

This result, which was derived by computing only the algebraic part of the \hbar^4 -term has been confirmed from a complete calculation of this correction.⁽²⁰⁾

Because of the classical collapse between opposite charges, the WK expansions for multicomponent systems with pure $1/r$ interactions cannot be properly defined. However, this difficulty is circumvented by introducing an arbitrary short-ranged regularization of the Coulomb potential. Then, the corresponding model is well-behaved in the classical limit with Maxwell–Boltzmann statistics. The particle correlations can be expanded in powers of \hbar^2 . As in the case of the OCP, the terms of order \hbar^2 are found to decay faster than any inverse power. On the contrary, all the higher order terms, starting from \hbar^4 , decay algebraically as $1/r^6$.⁽⁹⁾ This analysis is carried out in the framework of the Feynman–Kac representation. The basic mechanism is similar to that exhibited in the simple model of Section 2, where now all particles are replaced by filaments with interactions regularized at short distances.

3.2. Corrections to the RPA for the OCP

The OCP with Fermi statistics can be studied within the standard perturbation formalism.⁽²¹⁾ At finite temperature, the RPA correlations decay faster than any inverse power. However, there exist corrections to RPA which involve diagrams with two RPA interaction lines (see Fig. 7) that lead to a $1/r^{10}$ tail in the charge correlation.⁽¹¹⁾ In the semiclassical limit, the leading term in \hbar of this tail does coincide with the formula (3.1) obtained by a direct WK expansion. (The exchange contributions vanish

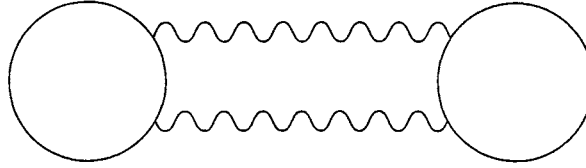


Fig. 7. A Feynman graph which leads to algebraic tails in the charge correlation. A wavy line represents the RPA potential. A circle represents a fermionic loop built with free propagators.

exponentially fast with respect to \hbar).⁽²²⁾ The above diagrams also provide algebraic tails at zero temperature, as noticed by several authors.^(23, 24) We mention that the oscillatory algebraic behavior of the RPA correlation at zero temperature⁽²⁵⁾ is due to the singularity of the Fermi distribution at the Fermi wave number. This effect disappears at finite temperature, and has nothing to do with the bad screening of the effective dipolar interactions described in Section 2 and responsible for the tails (2.12)–(3.1).

4. MULTICOMPONENT PLASMAS WITH QUANTUM STATISTICS AND PURE COULOMB INTERACTIONS

Now, we turn to the true problem, where quantum statistics are taken into account, and no arbitrary short-ranged regularization of the Coulomb potential is introduced. In Section 4.1, we present the loop formalism which arises from the Feynman–Kac representation. In Section 4.2, we sketch the diagrammatic resummations which are necessary because of the long range of the loop potential. The particle correlations are inferred from the resummed diagrammatic representation of the loop distribution functions in Section 4.3.

4.1. Loop Formalism

At the inverse temperature β , when a chemical potential μ_α is associated with each species α , and when the system is in a finite volume \mathcal{A} , the quantum grand partition function is

$$\Xi(\beta, \{\mu_\alpha\}, \mathcal{A}) = \sum_{N_\alpha} \prod_{\alpha} \exp(\beta\mu_\alpha N_\alpha) \text{Tr}_{\mathcal{A}} \exp(-\beta H_N) \quad (4.1)$$

where N_α runs from 0 to ∞ and H_N is the Hamiltonian given in (1.1). The trace is taken over a basis of quantum states which are symmetric with respect to permutations of the particles of the same species in the case of

bosons, and which are antisymmetric in the case of fermions. Thus, in space and spin representation, the trace gives rise to a sum over permutations of the particles of the same species.

Then, a notion of loops emerges from two properties. First, any permutation can be expressed uniquely as a product of cycles with no common element. Second, the noncommutativity between the kinetic and interaction quantum operators is circumvented by applying the Feynman–Kac formula to the diagonal and nondiagonal matrix elements which appear in the trace in (4.1). This representation introduces Brownian paths, as it has already been seen in the simple model of two quantum charges embedded in a classical plasma. Moreover, the Hamiltonian (1.1) does not depend on the spin, so that a loop involves only particles that have the same spin state. Henceforth, spins contribute only simple degeneracy factors.

The notion of loop is now illustrated in the case of 3 identical particles and of the permutation π such that $\pi(1) = 1$, $\pi(2) = 3$ and $\pi(3) = 2$. The path integral representation of the density-matrix element corresponding to the permutation π involves the Brownian paths $\omega_{i, \pi(i)}$, where $\omega_{i, \pi(i)}(s)$ is a Brownian path starting from \mathbf{r}_i at time $s = 0$ and ending at $\mathbf{r}_{\pi(i)}$ at time $s = 1$. Every Brownian path $\omega_{i, \pi(i)}(s)$ can be decomposed into a uniform motion on a straight line linking \mathbf{r}_i to $\mathbf{r}_{\pi(i)}$ plus a random contribution, namely,

$$\omega_{i, \pi(i)}(s) = (1 - s) \mathbf{r}_i + s \mathbf{r}_{\pi(i)} + \lambda_\alpha \xi_i(s) \quad (4.2)$$

In (4.2) $\xi_i(s)$ is the dimensionless Brownian bridge introduced in Section 2. The matrix element of $\exp(-\beta H_3)$ corresponding to the permutation π reads

$$\begin{aligned} & \langle \mathbf{r}_1 \mathbf{r}_3 \mathbf{r}_2 | \exp(-\beta H_3) | \mathbf{r}_1 \mathbf{r}_2 \mathbf{r}_3 \rangle \\ &= \frac{1}{(2\pi\lambda_\alpha^2)^{9/2}} \int \prod_{i=1}^3 \mathcal{D}(\xi_i) \exp\left(-\frac{(\mathbf{r}_2 - \mathbf{r}_3)^2}{\lambda_\alpha^2}\right) \\ & \quad \times \prod_{i < j} \exp\left[-\beta e_\alpha^2 \int_0^1 ds v_C(|\omega_{i, \pi(i)}(s) - \omega_{j, \pi(j)}(s)|)\right]. \end{aligned} \quad (4.3)$$

The contribution of the kinetic terms lie in the normalization factor $1/(2\pi\lambda_\alpha^2)^{9/2}$ factor and in the Gaussian measure of the dimensionless Brownian bridges ξ_i . The exchange in an ideal gas appears in the Gaussian term which depends on the distances between particles which are permuted directly together under a cycle. The interaction terms are disentangled from the kinetic terms and lie in a product where each term involves only one pair of Brownian paths. The interaction between two Brownian paths is the

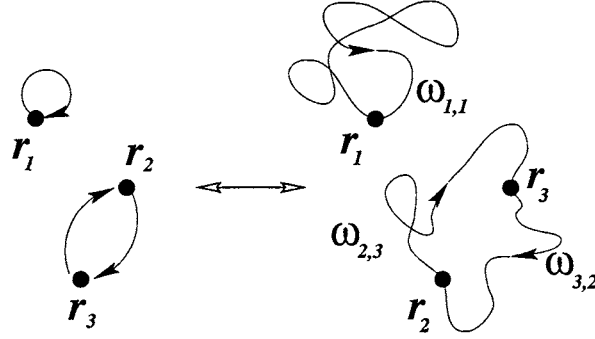


Fig. 8. Three quantum particles and their equivalent Brownian paths in the Feynman-Kac representation. On the left side, the arrows denote the permutation π involved in the corresponding matrix element of $\exp(-\beta H_3)$. On the right side, the Brownian paths $\omega_{i, \pi(i)}(s)$ are represented by lines that connect r_i to $r_{\pi(i)}$, ($i = 1, 2, 3$).

integral of the Coulomb interaction between line elements with the same time s , as has already been seen in the simple model of two quantum charges. More generally, a particle, such as particle 1, that is not exchanged with any other one in the density-matrix element, is associated with a closed filament, whereas p particles, such as particles 2 and 3, that are permuted with one another under a cyclic permutation are described, by p open filaments, which can be collected in a loop. Thus, every matrix element is exactly given by a Boltzmann factor corresponding to loops after functional integration over the loop shapes. This general equivalence is exemplified in Eq. (4.3) and is illustrated in Fig. 8.

Finally, the Feynman-Kac representation allows one to write the quantum grand partition function of the point particles as the Maxwell-Boltzmann grand partition function of a system of classical loops with random shapes and two-body interactions. This identity was first used in Statistical Mechanics by Ginibre,⁽²⁶⁾ in order to show that low-density expansions of thermodynamic functions are convergent for some class of integrable potentials. Recently, the interest of such a formulation has also been pointed out in a review paper by Høye and Stell.⁽²⁷⁾

In order to study the correlations, it is convenient to write the grand partition function as follows,⁽¹³⁾

$$\Xi_{loop} = \sum_{N=0}^{\infty} \frac{1}{N!} \int \prod_{n=1}^N [d\mathcal{L}_n z(\mathcal{L}_n)] \prod_{i < j} \exp[-\beta e_i e_j v(\mathcal{L}_i, \mathcal{L}_j)] \quad (4.4)$$

A loop \mathcal{L} is characterized by its position \mathbf{R} (the position of one of the particles involved in the loop) and its internal degrees of freedom: the

species α of the corresponding particles, the exchange degeneracy p of the loop (namely, the number of particles exchanged under the corresponding cyclic permutation), and the shape \mathbf{X} (the particle positions which are not equal to \mathbf{R} and the Brownian paths that connect them together). The integration over the loop variables $d\mathcal{L}$ is a summation over the species α and the exchange degeneracy p , and an integration over the position \mathbf{R} and the shape \mathbf{X} of the loop.

The loop fugacity $z(\mathcal{L})$ in (4.4) reads

$$z(\mathcal{L}) = (\pm 1)^{p-1} \frac{1}{p} (2S_\alpha + 1) \left[\frac{\exp(\beta\mu_\alpha)}{(2\pi\lambda_\alpha^2)^{3/2}} \right]^p \exp \left[- \sum_{i=1}^p \frac{(\mathbf{r}_{\pi(i)} - \mathbf{r}_i)^2}{2\lambda_\alpha^2} \right] \\ \times \exp[-\beta E_{self}(\alpha, p, \mathbf{X})]. \quad (4.5)$$

The *sign* in the first factor is $+$ in the case of bosons, and $-$ in the case of fermions. Thus, for fermions, the sign of the loop-fugacity depends on the number of particles involved in the loop. The factor $1/p$ arises from combinatorics; it is associated with the arbitrary choice of the position \mathbf{R} of the loop among the p particle positions involved in the loop. The factor $2S_\alpha + 1$ arises from spin degeneracy, because all particles in a loop are in the same spin state. The presence of p particles in the loop leads to the one-particle fugacity to the power p . The Gaussian describes the exchange in an ideal gas. Eventually, the self-energy E_{self} is the sum of the interactions between the open Brownian paths involved in the loop. The self-energy of a loop is positive, and the absolute value of the fugacity of interacting loops is lower than for noninteracting loops. In other words, the interaction between identical charges is repulsive and tends to reduce the importance of exchange effects.

The potential between loops in (4.4) is a two-body potential between extended objects. This potential is the sum of the interactions between the open Brownian paths belonging to different loops. Each interaction itself reduces to an equal-time average of the genuine Coulomb potential along the Brownian paths. We stress the following important point. The loop potential is different from the electrostatic potential between charged wires with the same shapes, as it was the case in the simple model of two quantum charges embedded in a classical bath. This will be crucial for the inhibition of the exponential clustering.

The main interest of the formula (4.4) is that the classical loops obey Maxwell-Boltzmann statistics and interact through a two-body potential. This nice formula, which is magic in some sense, is very convenient for the study of correlations. Indeed, by functional derivation of the grand partition function Ξ_{loop} with respect to the loop fugacities, we get the density

and correlations for loops. Moreover, these distribution functions can be represented by Mayer-like expansions in terms of the loop density $\rho(\mathcal{L})$. After integration over the internal degrees of freedom of the loops, except their species, we get the distribution functions for the quantum particles.

4.2. Diagrammatic Resummations of Loop-Density Expansions

The usual techniques of Mayer graphs introduced for point entities can be generalized to the system of extended loops, because the loops interact via a two-body potential. The loop correlations $\rho^T(\mathcal{L}, \mathcal{L}')$ are represented by Mayer series either in the fugacity $z(\mathcal{L})$ or in the loop-density $\rho(\mathcal{L})$ by virtue of the principle of topological reduction. The diagrammatic representation of $\rho^T(\mathcal{L}, \mathcal{L}')$ in terms of $\rho(\mathcal{L})$ is the most convenient for studying large-distance behavior. The corresponding Mayer graphs are defined with the usual topological prescriptions,^(28, 29, 30) and the Mayer bond reads

$$f(\mathcal{L}, \mathcal{L}') = \exp[-\beta v(\mathcal{L}, \mathcal{L}')] - 1. \quad (4.6)$$

At large distances, the extent of the loops become negligible with respect to the distance between loops, and the potential $v(\mathcal{L}, \mathcal{L}')$ behaves as the pure Coulomb $1/|\mathbf{R} - \mathbf{R}'|$ -interaction between the total charges of the loops, as if they were point charges. (The total charge of a loop is the sum of the charges of the corresponding particles.) The divergencies in the Mayer graphs, which are induced by the long-range Coulomb nature of the loop potential, are exactly and explicitly resummed⁽¹³⁾ by a generalization of the method developed by Meeron for classical plasmas.⁽³¹⁾

The resummed graphs contain three kinds of resummed bonds between loop variables. The first two are a charge-charge Debye-interaction bond and a charge-multipole Debye interaction bond. The monopole-monopole and monopole-multipole parts of the loop potential are exponentially screened, because they coincide with their electrostatics analogs, as already mentioned in Section 2.2. Therefore, both of these bonds decay exponentially. The screening length reduces to the Debye-Hückel value at low density, when exchange effects become negligible, namely in a classical regime. It tends to the *RPA* value at high density, in the quantum weak coupling regime.

The third dressed bond involves the contributions of quantum bound states at short distances and multipole-multipole interactions. In this dressed bond, there appears the difference between the loop potential and the electrostatic interaction between wires, as in the simple model of two quantum charges embedded in a classical plasma (see Eq. (2.7)). Thus the dressed bond decays algebraically at large distances, with a $1/r^3$ leading term analogous to a dipolar interaction, similar to the expression (2.10). Hence, the multipole-multipole interactions are partially screened.

4.3. Quantum Particle Correlations

The particle–particle correlations $\rho_{\alpha\gamma}^T(r)$ can be derived from both the loop density and the loop correlations by integration over the internal degrees of freedom. The contribution of $\rho(\mathcal{L})$ is obtained by fixing the position of the loop and the position of another particle involved in the loop. The loop density can be represented by resummed diagrammatic series in terms of the fugacities $z(\mathcal{L})$. Such resummations are similar to those described in Section 4.2. Then, the contribution of $\rho(\mathcal{L})$ to $\rho_{\alpha\alpha}^T(r)$ falls off faster than any inverse power law, when r goes to infinity. This fast decay comes from the Gaussian terms describing exchange in an ideal gas and from the Gaussian weight of the Brownian paths.

The contribution of $\rho^T(\mathcal{L}, \mathcal{L}')$ to $\rho_{\alpha\gamma}^T(r)$ is obtained by a reorganization of the resummed diagrammatics described in the previous section.⁽¹⁴⁾ The loop correlation itself decays as $1/|\mathbf{R} - \mathbf{R}'|^3$, because of the presence of the partially screened dipolar interactions. However, after integration over the internal degrees of freedom of \mathcal{L} and \mathcal{L}' , the rotational invariance of both quantum fluctuations and interactions together with the harmonicity of the Coulomb potential eventually enforce the quantum particle correlations to decay faster than $1/r^3$ ($r = |\mathbf{R} - \mathbf{R}'|$). The possible $1/r^4$ and $1/r^5$ algebraic tails vanish, by similar mechanisms to those described in the simple model (see Section 2). Thus, the leading algebraic tail in $\rho_{\alpha\gamma}^T(r)$ decays as

$$\rho_{\alpha\gamma}^T(r) \sim \frac{A_{\alpha\gamma}}{r^6} \quad (4.7)$$

This tail arises from the fluctuations of the partially screened dipolar interactions involved in the dressed bonds.

The present diagrammatic analysis also allows one to show that the particle–charge correlation decays only as $1/r^8$, as previously conjectured.⁽⁹⁾ Moreover, the charge–charge correlation falls off only as $1/r^{10}$, as in the case of the OCP (3.1). This cascade of powers 6, 8 and 10 is due, roughly speaking, to a memory of classical screening which is traced by the charge–charge and charge–multipole Debye bonds in the diagrammatics.⁽¹⁴⁾

Furthermore, the general formalism allows one to generate low-density expansions at finite temperature, namely in regimes of weak coupling and weak degeneracy.⁽¹⁵⁾ For instance, for a hydrogen plasma of electrons and protons, the low-density forms of the coefficients $A_{\alpha\gamma}$ are

$$A_{ep} \sim A_{pp} \sim A_{ee} \sim \rho^2 \frac{\beta^4 \hbar^4 e^4}{960} \left(\frac{m+M}{mM} \right) \quad (4.8)$$

when the density goes to zero.^(12, 15) Up to order $\rho^{5/2}$, the \hbar dependence of the coefficients $A_{\alpha\gamma}$ entirely arises from the bare fluctuations of charges. The effects of bound states and quantum statistics emerge only from the order ρ^3 on.

5. CONCLUSION

As a conclusion, the quantum fluctuations of dipolar-like interactions lead to internal correlations which behave as the square of $1/r^3$, namely $1/r^6$. This mechanism is indeed exhibited in the simple model, the semi-classical expansions and the complete diagrammatic analysis for the fully manybody quantum plasma. We stress that these dipolar interactions arise from the individual quantum fluctuations of each particle, independently of any recombination process. Indeed, they appear in the OCP where all particles repel one another. Furthermore, in physical situations in which atoms or molecules are present, the usual van der Waals forces are incorporated in the above mechanism. More precisely, their effect is to modify the amplitude of the considered fluctuations, as illustrated by general investigation of the resummed diagrammatics at the order ρ^3 and beyond. A model of four quantum charges⁽³²⁾ embedded in a classical bath exemplifies how van der Waals forces appear in the general algebraic tails.

We mention that, except for the solvable model of Section 2, the algebraic tails have been obtained through perturbative expansions with respect either to Planck's constant or to the density. Although these results strongly indicate the existence of non-exponential clustering in real Coulomb matter at finite temperature and finite density, they remain to be settled at a rigorous level, perhaps in the spirit of Ref. 33 for a simplified model.

Finally, we turn to the physical consequences of this algebraic screening. First, there remains a perfect screening of external charges by the quantum plasma, but the induced charge density in the presence of an external infinitesimal charge decays only as $1/r^8$. This can be shown from the diagrammatical analysis.⁽¹⁴⁾ In fact, Martin and Oguey have rigorously shown⁽³⁴⁾ that, under weak clustering assumptions on the imaginary time-displaced correlations, classical external charges are perfectly screened by quantum plasmas. The present algebraic tails suggest that these clustering assumptions are indeed satisfied.

Second, in order to estimate the quantitative importance of the algebraic tails, we consider the crossover distance r^* at which the algebraic tails dominate the classical exponential tails. In weakly coupled and weakly degenerated plasmas, these estimates can be obtained from the low-density expansions (see Section 4.3). For instance, in the hydrogen plasma in the

core of the Sun or in the charge-carrier gas in Germanium, r^* is found to be of the order of thirty to forty times the Debye screening length.^(12, 15) Of course, in other situations where quantum effects are more important, the exponential classical tails should be overcome at any scale. On the other hand, a relation between algebraic screening and dynamical effects might be found in solid state physics where the exchange effects are important. As mentioned in Section 3.2, there appear other sources of algebraic tails at zero temperature. Consequently, slower decays than $1/r^6$ might appear, for instance in the case of electrons in metals.

ACKNOWLEDGMENTS

F. C. was partially supported by the Région Rhône-Alpes. We thank the referees for valuable comments.

REFERENCES

1. F. J. Dyson and A. Lenard, *J. Math. Phys.* **8**, 423 (1967); **9**, 698 (1968).
2. J. L. Lebowitz and E. Lieb, *Adv. Math.* **9**, 316 (1972); E. H. Lieb, *Rev. Mod. Phys.* **48**, 553 (1976).
3. P. Debye and E. Hückel, *Phys. Z.* **9**, 185 (1923).
4. L. H. Thomas, *Proc. Camb. Phil. Soc.* **23**, 542 (1927); E. Fermi, *Z. Physik* **48**, 73 (1928); N. F. Mott, *Proc. Camb. Phil. Soc.* **32**, 281 (1936).
5. D. Pines and Ph. Nozières, *The Theory of Quantum Liquids* (Benjamin, New York, 1986).
6. D. C. Brydges and P. Federbush, *Commun. Math. Phys.* **73**, 197 (1980).
7. D. C. Brydges and P. Federbush, *Rigorous Atomic and Molecular Physics*, edited by G. Velo and A. S. Wightman (Plenum Press, New York, 1981).
8. D. C. Brydges and E. Seiler, *J. Stat. Phys.* **42**, 405 (1986).
9. A. Alastuey and Ph. A. Martin, *Phys. Rev. A* **40**, 6485 (1989).
10. A. Alastuey and Ph. A. Martin, *Europhys. Lett.* **6**, 385 (1988).
11. F. Cornu and Ph. A. Martin, *Phys. Rev. A* **44**, 4893 (1991).
12. F. Cornu, in *Physics of Strongly Coupled Plasmas*, ed. by W. D. Kraeft and M. Schlanges (World Scientific, Singapore, 1996).
13. F. Cornu, *Phys. Rev. E* **53**, 4562 (1996).
14. F. Cornu, *Phys. Rev. E* **53**, 4595 (1996).
15. F. Cornu, *Phys. Rev. Lett.* **78**, 1464 (1997).
16. Ph. A. Martin, *Rev. Mod. Phys.* **60**, 1075 (1988).
17. E. H. Lieb and H. Narnhofer, *J. Stat. Phys.* **12**, 291 (1975); *J. Stat. Phys.* **14**, 465 (1976).
18. See, e.g., A. Alastuey, *Annales de Physique* (Paris) **11**, 653 (1986).
19. B. Jancovici, *Mol. Phys.* **32**, 1177 (1976).
20. M. M. Gombert and D. Léger, *Phys. Lett. A* **185**, 417 (1994).
21. See, e.g., A. L. Fetter and J. D. Walecka, *Quantum Theory of Many Particle Systems* (McGraw-Hill, New York, 1971); J. W. Negele and H. Orland, *Quantum Many-Particle Systems*, in *Frontiers in Physics*, vol. 68 (Addison-Wesley, 1988).
22. B. Jancovici, *Physica* **91A**, 152 (1978).
23. A. C. Maggs and N. W. Ashcroft, *Phys. Rev. Lett.* **59**, 113 (1987).

24. D. C. Langreth and S. H. Vosko, *Phys. Rev. Lett.* **59**, 497 (1987).
25. J. Friedel, *Phil. Mag.* **43**, 153 (1952); *Nuovo Cimento* **7** Suppl. 2, 287, (1958).
26. J. Ginibre, *J. Math. Phys.* **6**, 238 (1965); *J. Math. Phys.* **6**, 252 (1965); *J. Math. Phys.* **6**, 1432 (1965); in *Statistical Mechanics and Quantum Field Theory*, 1971 Les Houches Lectures, ed. by C. de Witt and R. Stora (Gordon and Breach, New York, 1971).
27. J. S. Høye and G. Stell, *J. Stat Phys.* **77**, 361 (1994).
28. J. E. Mayer and M. G. Mayer, *Statistical Mechanics* (Wiley, New York, 1940); J. E. Mayer and E. Montroll, *J. Chem. Phys.* **9**, 2 (1941).
29. T. Morita and K. Hiroike, *Prog. Theor. Phys.* **25**, 537 (1961).
30. See, e.g., J. P. Hansen and I. R. McDonald, *Theory of Simple Liquids* (Academic Press, London, 1976).
31. E. Meeron, *J. Chem. Phys.* **28**, 630 (1958); *Plasma Physics* (Mc Graw-Hill, New York, 1961).
32. Ph. A. Martin, to be published.
33. D. C. Brydges and G. Keller, *J. Stat. Phys.* **76**, 285 (1994).
34. Ph. A. Martin and Ch. Oguey, *Phys. Rev. A* **33**, 4191 (1986).